MRS Communications (2013), *3*, 241–244

doi:10.1557/mrc.2013.37

MRS Communications

Research Letters

Elucidating the kinetics of twin boundaries from thermal fluctuations

Dengke Chen and **Yashashree Kulkarni,** Department of Mechanical Engineering, University of Houston, Houston, Texas 77204
Address all correspondence to Yashashree Kulkarni at **ykulkarni@uh.edu**

(Received 5 June 2013; accepted 9 September 2013)

Abstract

There is compelling evidence for the critical role of twin boundaries (TBs) in imparting the extraordinary combination of strength and ductility to nanotwinned metals. Here, we investigate the thermal fluctuations of TBs in face-centered-cubic metals to elucidate the deformation mechanisms governing their kinetic properties using molecular dynamics simulations. Our results show that the TB motion is strongly coupled to shear deformation up to 0.95 homologous temperature. A rather unexpected observation is that coherent TBs do not exhibit any capillarity-induced fluctuations even at high temperatures, in sharp contrast to other high-angle grain boundaries.

Nanotwinned metals are known to demonstrate a remarkable combination of mechanical properties, namely, ultra-high strength, enhanced ductility, and high strain rate sensitivity.[1–6] This is in contrast to nanocrystalline materials, which exhibit a loss of ductility, and grain stability with decreasing grain size, thereby offsetting the initial excitement generated by their very high yield strength (see[7] for review). It is well documented, through many experimental and theoretical studies, that this loss of stability of nanograined metals, which has severely limited their practical application, is associated with thermally-activated or stress-assisted grain growth caused by grain boundary (GB)-mediated processes such as migration and sliding.[8–11] It is natural then, that the grain growth and twin lamella stability in nanotwinned metals would also be intimately connected to the thermodynamic and kinetic properties of twin boundaries (TBs) and GBs. Although the prospect of the stability of nanotwinned structures is of vital concern, one which defines their ultimate utility and raises fundamental questions regarding the underlying physics, the issue has remained relatively unaddressed until recently.[12,13]

In this Research Letter, we report our investigation of the motion of TBs by atomistic modeling of their thermal fluctuations over a range of temperatures. In the theory of statistical mechanics of interfaces, thermal fluctuations have been effectively used to elucidate the thermodynamic and kinetic properties of fluid and solid membranes and interfaces.[14] In the case of high-angle GBs, the capillary wave theory has been successfully applied to relate their long wavelength thermal fluctuations to important quantities such as the GB stiffness and mobility.[15] According to the capillarity theory, the energetic cost for these out-of-plane fluctuations is attributed to the surface tension, or in other words, the increase in the area of the interface to accommodate the bending due to fluctuations. The Fourier spectrum of these capillarity-induced fluctuations is given by

$$\langle |A(k)|^2 \rangle = \frac{k_B T}{S \Gamma k^2}, \tag{1}$$

where k is the wave vector, $A(k)$ is the amplitude of the mode k fluctuation, S is the area of the interface or gain boundary, and Γ is the interfacial stiffness. The initial aim of our work was to furnish a constitutive description for TBs based on this relation. However, as described in what follows, our molecular dynamics simulations revealed that a fluctuating TB, unlike other high-angle GBs, does not follow the relation in Eq. (1), even at very high temperatures. In fact, our observation that the TBs show $1/k$ dependence of the fluctuation average and consequently, do not show capillarity-induced fluctuations, was not obvious to us when we started the study and has not been reported in the literature before. While this study was ongoing, a paper by Karma et al.[16] appeared, which investigated the fluctuations of low-angle GBs and proposed the relation between the $1/k$ dependence of equilibrium fluctuations of low-angle GBs and their kinetics via shear-coupled motion. In this paper, we present our thermal fluctuation simulations for TBs, interpret them within the context of this recent work by Karma et al.[16] as well as discuss the relevance of this study within the current literature on TBs and nanotwinned metals.

The TB fluctuations were modeled by molecular dynamics simulations using Large-scale Atomic/Molecular Massively Parallel Simulator (LAMMPS).[17] All of the simulations were performed on Cu using the embedded-atom method developed by Mishin et al.[18] At each temperature, the simulation cell was first equilibrated for 100 ps at zero pressure using the NPT ensemble. The molecular dynamics run was then conducted for 1 ns under the NVT ensemble using the Nose–Hoover thermostat. The system configuration was

observed at every 1000 time steps. To investigate the effect of temperature on the fluctuations, the simulations were conducted over temperatures ranging from 100 to 1300 K. The simulation box dimensions were $L_x \approx 300$ Å, $L_y \approx 100$ Å, and $L_z \approx 20$ Å with periodic boundary conditions in the x- and z (lateral)-directions as shown in Fig. 1. The specimen was oriented along the $[\bar{1}12]$, $[\bar{1}1\bar{1}]$, and $[\bar{1}\bar{1}0]$ crystallographic directions. Since the cell dimension was much smaller in the z-direction, the fluctuations along this direction were neglected. The y-direction was aligned normal to the TB, and the fluctuations were observed along the x-direction. To assess the effect of cell size on the fluctuation measurements, we also performed the simulation at 1000 K on a larger specimen with dimensions 600 Å × 200 Å × 40 Å. The results changed only negligibly confirming that our initial choice of dimensions was appropriate for extracting the thermal fluctuations of a single interface.

At 0 K, the TB is a flat interface located at the center of the simulation box as shown by the dotted lines in Fig. 1. At finite temperature, the interface fluctuates and we denote the instantaneous out-of-plane displacement by $h(x)$. Figure 2 shows the atomistic structure of a fluctuating TB at an instant with red atoms being the farthest distance above the initial flat configuration and blue atoms being the lowest. Many approaches have been proposed to locate the instantaneous position of a fluctuating interface in molecular dynamics simulations.[15,19–22] In this work, we used the centrosymmetry parameter to distinguish between atoms belonging to the interface and the bulk and thus, identify the instantaneous TB position. The centrosymmetry parameter of an atom is defined as

$$CS = \sum_{i=1}^{N/2} |\,\mathbf{R}_i + \mathbf{R}_{i+N/2}\,|^2, \tag{2}$$

where N is the number of nearest neighbors and equals 12 for face-centered-cubic (fcc) crystals. $\mathbf{R}_i$ and $\mathbf{R}_{i+N/2}$ are vectors from the central atom to a particular pair of nearest neighbors. For a perfect crystal region, CS is zero; for defects such as a dislocation, GB, or surface, it is a finite real number. Since the fluctuation could be ignored in the z-direction, CS did not change significantly in this direction and hence, was summed along this direction. To obtain a smooth curve for the variation of CS along the y-direction to identify the interface position, the simulation cell was divided into many slices along the x-direction as shown in Fig. 3. Within each slice, this local parameter CS was extracted as the average

$$\overline{CS}(x, y) = \sum_i \frac{CS_i}{(y_i - y)^2 + 1} \tag{3}$$

based on the method proposed by Trautt and Upmanyu.[20] CS_i denotes the centrosymmetry parameter of atom i and y_i is the y-coordinate of atom i. Then, the average centrosymmetry function, $\overline{CS}$, for each slice, depends on y, and can be plotted for any particular slice along the x-direction. The peak corresponds to the instantaneous location of the TB in this slice. Following a similar procedure for each slice, the profile of the function $h(x)$ can be obtained. The Fourier transform of $h(x)$ is given by

$$h(x) = \sum_k A(k)\, e^{ikx}. \tag{4}$$

Assuming the simulation cell to be divided into N slices labeled as x_i, $i = 0,1,2, \ldots, N-1$, the fluctuation spectrum $A(k)$ was obtained as the discrete Fourier transform

$$A(k) = \frac{1}{N} \sum_{i=0}^{N-1} h(x_i) \exp\left(-2\pi k \frac{i}{N}\right). \tag{5}$$

Once the fluctuation amplitude $A(k)$ was computed for a given snapshot of the interface, the fluctuation average, $\langle |A(k)|^2 \rangle$ was determined by computing the average over the snapshots taken at every 1000 time steps during the simulation.

Figure 4 shows the results for the variation of the power spectrum, $\langle |A(k)|^2 \rangle$, with k for different temperatures on a log-log plot. We observe that $\langle |A(k)|^2 \rangle$ has a linear dependence on $1/k$ all the way up to the 0.95 homologous temperature. Within the context of the existing literature on thermal fluctuations of low-angle GBs and high-angle GBs, this is a rather unexpected behavior of coherent TBs.

As mentioned earlier, several molecular dynamics studies have revealed that many high-angle GBs follow the relation described by Eq. (1), exhibiting a $1/k^2$ dependence of the fluctuation spectrum. However, based on a dislocation model, Rottman[23] predicted that the energy of the thermal fluctuations of low-angle GBs is linear in wave number, thereby implying a $1/k$ dependence of $\langle |A(k)|^2 \rangle$. A very recent work by Karma et al.[16] provides a fresh insight into the deformation mechanisms that lead to these differences in the fluctuation spectra for low-angle and high-angle GBs. They show that the $1/k$ scaling behavior is associated with shear-coupled motion of GBs, and is exhibited by low-angle GBs even at high temperatures. They derive the relation between

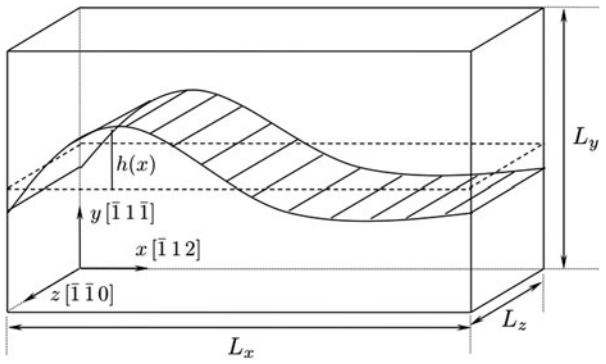

Figure 1. Schematic of the bicrystal specimen showing the flat TB at 0 K (dotted lines) and the fluctuating TB at finite temperature (solid lines).

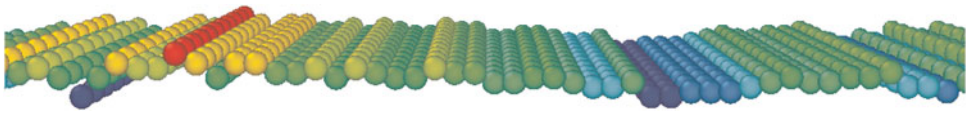

Figure 2. Atomistic structure of a section of a fluctuating TB at an instant. The colors represent the distance of the atoms above (red) and below (blue) the initial flat configuration. The fluctuations have been exaggerated for illustration.

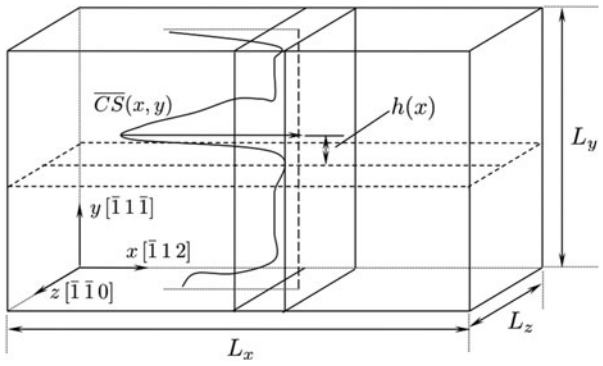

Figure 3. Schematic of the bicrystal showing the variation of the average centrosymmetry parameter, $\overline{CS}$ in a slice along the *x*-axis. This is used to identify the instantaneous position of the TB during the simulation.

equilibrium fluctuations and the coupling factor as

$$\langle |A(k)|^2 \rangle = \frac{k_B T}{C\beta^2 k}, \tag{6}$$

where C is a parameter comprising of the elastic constants of the material, while $\beta = v_{||}/v_n$ was defined by Cahn et al.[24] as the coupling factor between the applied shear velocity ($v_{||}$) and the resulting normal GB velocity (v_n). In contrast to low-angle GBs, high-angle GBs exhibit a $1/k^2$ scaling law at high

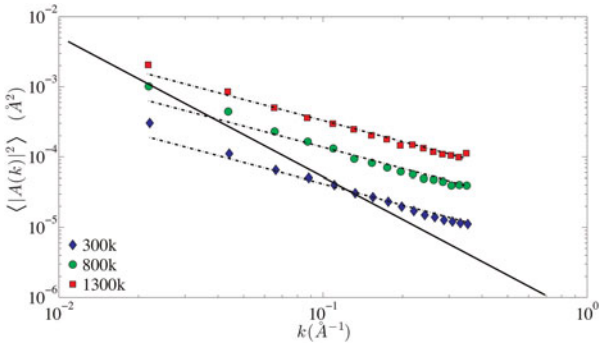

Figure 4. Power spectrum of TB fluctuations as a function of *k* for different temperatures obtained by molecular dynamics simulations. The dashed lines indicate trend lines obtained for each curve by the least squares method. The slope of all of the three dashed lines is −1. The solid line with slope −2 is shown for reference.

temperatures attributed to capillarity-induced fluctuations, and a $1/k$ dependence at low temperatures. This transition is associated with a transition in the kinetics of the GBs from shear coupling to pure sliding. The same conclusions were drawn by Cahn et al.[24] based on their molecular dynamics simulations of shear deformation of bicrystals with various low-angle and high-angle GBs. At low and intermediate temperatures, the normal motion of all of the GBs was coupled to shear deformation. However, at high temperatures, the high-angle GBs showed a transition to pure sliding and spontaneous normal motion and the shear coupling vanished, while the low-angle GBs still retained their coupled response up to near the melting point.

Taken together, our simulations show that coherent TBs do not exhibit any capillarity-induced fluctuations even at high temperatures, in sharp contrast to other high-angle GBs. In fact, the thermal fluctuations indicate that the TB motion remains strongly coupled to shear deformation up to 0.95 homologous temperature. These conclusions are also in agreement with our prior simulations of the high-temperature shearing of twinned bicrystals in which we observed that, unlike many high-angle GBs studied by Cahn et al.,[24] the TBs do not exhibit sliding or spontaneous normal motion at high temperatures.[25] Furthermore, Fig. 4 shows that the intercept of the $\langle |A(k)|^2 \rangle$ plot increases with temperature. Taking the log of Eq. (6), we have the expression for the intercept as $\log(k_B T/C\beta^2)$. Since β is essentially a geometric parameter as discussed by Cahn et al.,[24] and C would decrease with temperature due to softening, the intercept should increase with temperature. Thus, our atomistic simulations show a qualitative agreement with the theoretical model by Karma et al.[16] for the temperature dependence of the thermal fluctuations of the TBs.

In summary, our study provides insights into the thermal fluctuations of TBs and relates them to their kinetics and the high temperature stability of nanotwinned structures. Although it is well established that the TBs exhibit low mobility and migration in the absence of applied shear stress, we draw these conclusions from the nature of their thermal fluctuations. Based on the recent work by Karma et al.,[16] which establishes the relation between the $1/k$ dependence of equilibrium fluctuations of low-angle GBs and their kinetics via shear-coupled motion, we show that the same behavior also extends to TBs even up to near the melting point. While nanocrystalline materials are known to be prone to grain growth and creep due to GB normal motion and GB sliding, respectively, our simulations support that the TBs do not exhibit sliding or

spontaneous normal motion and hence predict stable twin lamella at high temperatures. This is in qualitative agreement with the recent experimental studies by Bezares et al.,[13] which reveals enhanced stability of nanotwinned fcc metals under nanoindentation and creep tests compared with their nanocrystalline counterparts. However, more detailed simulations of nanotwinned structures are needed to shed light on the interplay of GBs and TBs and determining the overall grain stability as well as the effect of pre-existing defects in these interfaces, which will be pursued in our future work.

Acknowledgments

The authors would like to acknowledge the support of the US National Science Foundation under grants DMR-1006876 and CMMI-1129041 and the Defense Advanced Research Projects Agency under grant N66001-10-1-4033. Yashashree Kulkarni would like to thank Professor Pradeep Sharma, University of Houston, for stimulating discussions. The simulations were performed on the supercomputing facility hosted by the Research Computing Center at University of Houston.

References

1. L. Lu, Y. Shen, X. Chen, L. Qian, and K. Lu: Ultrahigh strength and high electrical conductivity in copper. *Science* **304**, 422 (2004).
2. A.M. Hodge, Y.M. Wang, and T.W. Barbee Jr.: Mechanical deformation of high-purity sputter-deposited nano-twinned copper. *Scr. Mater.* **59**, 163 (2008).
3. D. Jang, X. Li, H. Gao, and J.R. Greer: Deformation mechanisms in nanotwinned metal nanopillars. *Nature Nanotech.* **7**, 594 (2012).
4. A.J. Cao, Y.G. Wei, and X.S. Mao: Deformation mechanisms of face-centered-cubic metal nanowires with twin boundaries. *Appl. Phys. Lett.* **90**, 151909 (2007).
5. R.J. Asaro and Y. Kulkarni: Are rate sensitivity and strength effected by cross-slip in nano-twinned FCC metals. *Scr. Mater.* **58**, 389 (2008).
6. T. Zhu, J. Li, A. Samanta, H.G. Kim, and S. Suresh: Interfacial plasticity governs strain rate sensitivity and ductility in nanostructured metals. *Proc. Natl. Acad. Sci. USA* **104 (**2007).
7. M. Dao, L. Lu, R.J. Asaro, J.T.M. De Hossan, and E. Ma Li: Toward a quantitative understanding of mechanical behavior of nanocrystalline metals. *Acta Mater.* **55**, 4041 (2007).
8. D. Wolf, V. Yamakov, S.R. Phillpot, A. Mukherjee, and H. Gleiter: Deformation of nanocrystalline materials by molecular-dynamics simulation: relationship to experiments? *Acta Mater.* **53**, 1 (2005).
9. K. Zhang, J.R. Weertman, and J.A. Eastman: Rapid stress-driven grain coarsening in nanocrystalline Cu at ambient and cryogenic temperatures. *Appl. Phys. Lett.* **87**, 061921 (2005).
10. F. Sansoz and V. Dupont: Grain growth behavior at absolute zero during nanocrystalline metal indentation. *Appl. Phys. Lett.* **89**, 111901 (2006).
11. X. Li, Y. Wei, W. Yang, and H. Gao: Competing grain boundary and dislocation mediated mechanisms in plastic strain recovery in nanocrystalline aluminum. *Proc. Natl. Acad. Sci. USA* **106**, 16108 (2009).
12. C.J. Shute, B.D. Myers, S. Xie, T.W. Barbee Jr., A.M. Hodge, and J.R. Weertman: Detwinning, damage and crack initiation during cyclic loading of Cu samples containing aligned nanotwins. *Scr. Mater.* **60**, 1073 (2011).
13. C.J. Bezares, S. Jiao, Y. Liuc, D. Bufford, L. Lu, X. Zhang, Y. Kulkarni, and R.J. Asaro: Indentation of Nano-Twinned FCC Metals: Implications for Nano-Twin Stability. *Acta Mater.* **60**, 4623 (2012).
14. S.A. Safran: *Statistical Thermodynamics of Surfaces, Interface, and Membranes* (Westview Press, Colorado, USA, 2003).
15. J.J. Hoyt, Z.T. Trautt, and M. Upmanyu: Fluctuation in molecular dynamics simulation. *Math. Comput. Simul.* **80**, 1382 (2010).
16. A. Karma, Z.T. Trautt, and Y. Mishin: Relationship between equilibrium fluctuations and shear-coupled motion of grain boundaries. *Phys. Rev. Lett.* **109**, 095501 (2012).
17. S.J. Plimpton: Fast parallel algorithms for short-range molecular dynamics. *J. Comput. Phys.* **117**, 1 (1995).
18. Y. Mishin, M.J. Mehl, D.A. Papaconstantopoulos, A.F. Voter, and J.D. Kress: Structural stability and lattice defects in copper: ab initio, tight-binding, and embedded atom calculations. *Phys. Rev. B* **63**, 224106 (2001).
19. J.J. Hoty, M. Asta, A. Karma: Method for computing the anisotropy of the solid- liquid interfacial free energy. *Phys. Rev. Lett.* **86**, 5530 (2001).
20. Z.T. Trautt and M. Upmanyu: Direct two-dimensional calculations of grain boundary stiffness. *Scr. Mater.* **86**, 5530 (2001).
21. S.M. Foiles and J.J. Hoyt: Computation of grain boundary stiffness and mobility from boundary fluctuations. *Acta Mater.* **54**, 3351 (2006).
22. J.J. Hoyt, Z.T. Trautt, and M. Upmanyu: Interface mobility from interface random walk. *Science* **314**, 632 (2006).
23. C. Rottman: Thermal fluctuation in low-angle grain boundary. *Acta Metall.* **34**, 2465 (1986).
24. J.W. Cahn, Y. Mishin, and A. Suzuki: Coupling grain boundary motion to shear deformation. *Acta Mater.* **54**, 4953 (2006).
25. T. Sinha and Y. Kulkarni: Anomalous deformation twinning in fcc metals at high temperatures. *J. Appl. Phys.* **109**, 114315 (2011).